

# Distance-Aware Multi-Carrier (DAMC) Modulation in Terahertz Band Communication

Chong Han and Ian F. Akyildiz

Broadband Wireless Networking Laboratory  
 School of Electrical and Computer Engineering  
 Georgia Institute of Technology, Atlanta, Georgia 30332, USA  
 Email: {chong.han, ian}@ece.gatech.edu

**Abstract**—Terahertz Band (0.1-10 THz) communication is envisioned as a key technology to satisfy the increasing demand for ultra-broadband wireless communication. THz Band communication will alleviate the spectrum scarcity and capacity limitations of current wireless systems, and enable new applications both in classical networks and novel nanoscale networks. In this paper, a novel distance-aware multi-carrier (DAMC) modulation scheme is developed for both single-transmitter single-receiver and single-transmitter multiple-receiver cases in THz Band communication. The developed DAMC modulation scheme takes advantage of the distance- and frequency-dependent channel peculiarities, and provides adaptive utilization of the ultra-broad bandwidth in the THz Band. Furthermore, the data rates of the DAMC scheme are analytically investigated, numerically evaluated, and compared with existing single-band pulse-based modulation and fixed-bandwidth adaptive modulation. The results show that data rates can be improved by one order of magnitude by using the DAMC scheme, at the costs of design complexity for the control unit, multi-carrier modulator and channel feedback path.

**Index Terms**—Terahertz Band, Multi-carrier, Modulation, Ultra-broadband communication

## I. INTRODUCTION

Wireless data traffic has exponentially grown in the past years, and this has been accompanied by an increasing demand for higher data rates. In particular, wireless data rates have doubled every eighteen months over the last three decades and are currently approaching the capacity of wired communication systems [1], [2]. Following this trend, data rates reaching Terabit-per-second (Tbps) will be realized within the next five to ten years. Enormous bandwidth will be required to support the high data rates for the future ultra-broadband wireless communication and, amongst others, the Terahertz Band (0.1 – 10 THz) is identified as one of the promising spectrum bands [3], [4].

Compared to 60 GHz [5] or ultra-wideband (UWB) [6] systems, the bandwidth in the THz Band is ultra-broad, which ranges from several GHz to THz [7]. In terms of higher frequency bands, although infrared (IR) systems have high center frequencies and large available bandwidth, the IR technology has limited data rates due to poor sensitivity of incoherent receivers, high diffuse reflection losses, and limited power budget due to eye-safety limits [8].

The technology required to make THz Band communication reality is rapidly advancing. For the time being, both photonic

or optoelectronic [9], [10] and fully electronic transceivers based on Silicon-Germanium technology [11] have been investigated. In addition, Gallium-Nitride-based power amplifiers are being studied to increase the front-end power amplification for THz Band communication [12]. These, as well as novel nanomaterials such as graphene [13], [14], make the development of compact and energy-efficient THz Band transceivers and antennas feasible in the near future.

By enabling ultra-broadband communication in the THz Band, the spectrum scarcity and capacity limitations of current cellular systems can be addressed, and a plethora of applications can be boosted, which includes ultra-fast massive data transfers among nearby devices, or ultra-broadband small cell systems, or ultra-high-definition content streaming in advanced cellular networks. In addition, the THz Band will also enable novel networking applications at the nanoscale for biomedical and military industries [15], [16].

Although classical modulation schemes can be used at Terahertz frequencies, they cannot fully benefit from the properties of the THz Band [17]. The distance- and frequency-dependent peculiarities of the channel motivate the development of novel modulation schemes for THz Band communication. Recently, a novel single-band pulse-based communication scheme for nanoscale THz Band communication has been proposed [18]. However, this modulation is mainly valid for very short transmission distances, e.g. nanonetworks, in which molecular absorption does not drastically impact on the channel. In macroscale THz Band communication, molecular absorption defines multiple transmission windows, and each window has different available bandwidth ranging from several GHz to THz. Furthermore, the ultra-broad bandwidth associated to these transmission windows drastically changes with small variations in the communication distance.

For this, in our paper, we develop a distance-aware multi-carrier (DAMC) modulation scheme, which can take advantage of the distance- and frequency-dependent transmission windows, and provide adaptive utilization of the ultra-broad bandwidth in the THz Band. The DAMC scheme is realized in a control unit, which operates as follows. First, the transmitter identifies and selects the available transmission windows based on the communication distance. Second, each window is divided into many non-overlapping sub-windows, which are

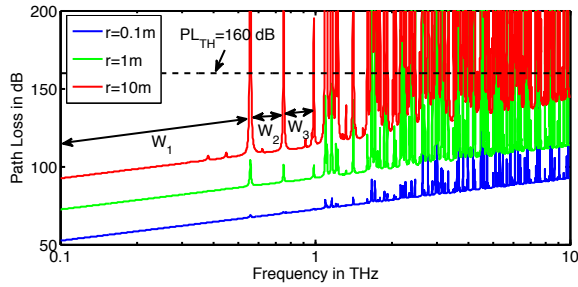


Figure 1: The distance- and frequency-dependent transmission windows in the THz Band channel [7].

used to transmit multi-carrier signals. Third, each carrier signal is modulated with a MQAM modulation, where the order,  $M$ , is chosen to satisfy the bit error rate (BER) and transmit power requirements at the receiver. The results show that data rates can be improved by one order of magnitude by using the DAMC scheme, at the costs of design complexity for the control unit, multi-carrier modulator and channel feedback path.

The main contributions of our work can be summarized as follows.

- We review the distance- and frequency-dependent peculiarities of the THz Band channel, and define the path loss threshold which is used to identify transmission windows.
- We develop the DAMC modulation scheme for both single-transmitter single-receiver (STSR) and single-transmitter multiple-receiver (STMR) cases in THz Band communication.
- We analytically investigate the data rates of the DAMC modulation scheme, and provide extensive numerical evaluation in both STSR and STMR communication.
- We compare our DAMC scheme with the single-band pulse-based communication and fixed-bandwidth adaptive modulation in the STSR case.

The remainder of this article is organized as follows. In Section II, we define the path loss threshold to identify transmission windows in the THz Band. In Section III, we develop the DAMC modulation scheme in the THz Band and analytically investigate the data rates. In Section IV, we numerically analyze the data rates of the DAMC scheme in both STSR and STMR networks. Finally, we conclude the paper in Section V.

## II. TRANSMISSION WINDOWS IN THE TERAHERTZ BAND

The total path loss in the THz Band channel mainly consists of the spreading loss and molecular absorption loss. Figure 1 shows the total path loss in the THz Band for different distances, which has been characterized in [7]. The path loss peaks caused by molecular absorption naturally create transmission windows, e.g.,  $w_1, w_2, w_3$ , amongst others. Each window has different bandwidth, which drastically changes with small variations in the communication distance.

These channel peculiarities motivate the development of novel distance-aware modulation schemes for THz Band com-

$r = 0.1 \text{ m}$	$r = 1 \text{ m}$	$r = 10 \text{ m}$
0.10 - 4.511 THz	0.10 - 1.659 THz	0.10 - 0.552 THz
4.514 - 6.074 THz	1.674 - 1.713 THz	0.562 - 0.748 THz
6.079 - 6.829 THz	1.721 - 2.162 THz	0.756 - 0.984 THz
6.832 - 7.612 THz	2.167 - 2.194 THz	0.991 - 1.086 THz
7.616 - 9.082 THz	2.198 - 2.219 THz	1.120 - 1.147 THz

Table I: The first five transmission windows for communication at 0.1m, 1m and 10m.

munication. However, in order to best utilize the ultra-broad bandwidth in the THz Band, there is a need for an analytical investigation on the distance-dependence of transmission windows, in which modulation schemes operate.

We define the *path loss threshold*,  $PL_{TH}$ , as the maximum path loss value that can be tolerated for transmission. Above this threshold, the frequency bands are not used in our design. An analytical solution to the path loss threshold in dB can be obtained by solving the link budget equation, as

$$PL_{TH} = P_T + G_T + G_R - P_R, \quad (1)$$

where  $P_T$  and  $P_R$  stand for the transmit power and receive power,  $G_T$  and  $G_R$  denote the transmit and receive antenna gain, respectively. In addition,  $P_R = \gamma + P_w$ , where  $\gamma$  is the signal-to-noise ratio (SNR) in dB, and  $P_w$  represents the total noise power at the receiver.

In THz Band communication, highly directional antennas or antenna arrays are advocated to overcome the very high path loss [17]. Therefore, we consider  $G_T = G_R = 30 \text{ dB}$ ,  $P_T = 10 \text{ dBm}$ ,  $\gamma = -10 \text{ dB}$  and  $P_w = -80 \text{ dBm}$  [15]. The resulting maximum path loss value is computed as  $PL_{TH} = 160 \text{ dB}$ , which will be used throughout our analysis.

Next, the available transmission windows are identified by having smaller path loss values than the path loss threshold, as shown in Table I. The transmission windows have strongly distance- and frequency-dependent bandwidth, which ranges from several GHz to THz. In particular, the first transmission window is 4.411 THz wide when  $r = 0.1 \text{ m}$ , while it shrinks to 1.559 THz and 0.452 THz for distances at 1 m and 10 m, respectively. There are 6 transmission windows for  $r = 0.1 \text{ m}$ , and the total aggregated bandwidth is 9.87 THz. By contrast, there are 98 non-consecutive transmission windows for  $r = 10 \text{ m}$ , while the total available bandwidth decreases to 5.90 THz.

The increase of communication distances leads transmission windows to dwindle their bandwidth, and even become unavailable (i.e., bandwidth shrinks to zero). This motivates the design of distance-aware (i.e., bandwidth-adaptive) modulation.

## III. DISTANCE-AWARE MULTI-CARRIER (DAMC) MODULATION

In light of the behavior of the THz Band channel, we develop the distance-aware multi-carrier modulation scheme, which can take advantage of the distance- and frequency-dependent transmission windows, and provide adaptive utilization of the ultra-broad bandwidth.

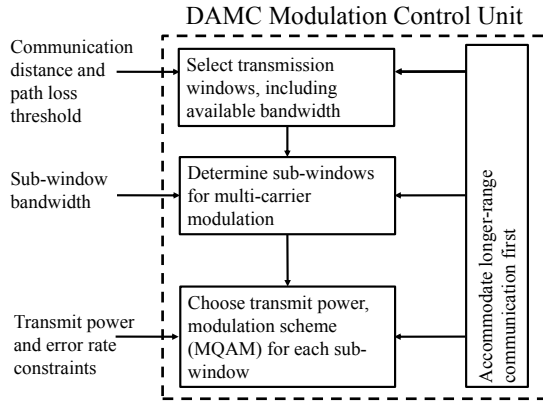


Figure 2: Architecture of the DAMC modulation control unit in THz Band communication.

*Orthogonal frequency division multiplexing* (OFDM) is suggested for 60 GHz systems to enhance the spectral efficiency [19]. However, the bandwidth is not scarce in the THz Band. Furthermore, the very complex transceivers, high peak-to-average power ratio (PAPR), and strict requirements for frequency synchronization make OFDM very challenging in the THz Band, where digital processors that can handle such very high data rates (e.g., over 1 Tbps) do not exist to date.

Instead, *multi-carrier modulation* in the DAMC scheme permits adaptive transmissions of different symbols on non-overlapping and equally spaced *sub-windows* in parallel. As a result, each carrier occupies smaller bandwidth and supports slower data rates. This effectively relaxes the design requirements of individual carriers, and is helpful for THz Band communication to process very high data rates. Nevertheless, many parallel modulators for different carriers and very fast signal generator to switch between carriers, are required to support multi-carrier modulation [20], [21].

The number of carriers is equal to the ratio between the total aggregated bandwidth and the bandwidth of each sub-window. Small sub-window bandwidth results in a large number of carriers, which reduces the complexity on each carrier and enhances the system capability to support high data rates. However, many carriers in parallel increase the complexity of the multi-carrier modulator design. This study of the optimal bandwidth of sub-windows is beyond the scope of this paper, and in this work, we consider  $B_g = 1$  GHz.

In the following, we develop the DAMC modulation scheme, to dynamically adapt the data rates and power on each sub-windows, for both *single-transmitter single-receiver* (STSR) and *single-transmitter multiple-receiver* (STMR) cases in THz Band communication.

#### A. STSR Communication

The operation of the developed DAMC modulation scheme is realized in a control unit as shown in Figure 2. In STSR communication, the DAMC scheme consists of three steps, as follows.

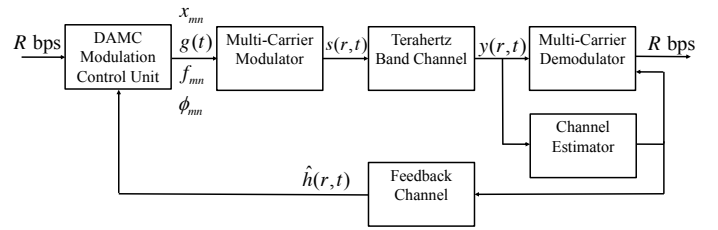


Figure 3: The system model of DAMC modulation communication.

- 1) At a given communication distance and a path loss threshold value, we select the transmission windows and obtain the available bandwidth, which are explained in Section II. The adaptive modulation requires a feedback path between the transmitter and receiver for the channel estimation.
- 2) The DAMC modulation scheme further divides the transmission windows into many non-overlapping sub-windows for multi-carrier modulation.
- 3) According to total transmit power and targeted error rate constraints, we can adaptively modulate the information and allocate transmit power to each sub-window, in order to maximize the data rate. The DAMC modulation control unit determines the modulation schemes (e.g., MQAM), multi-carrier frequencies and phases, which are used to generate the transmitted signal on the selected sub-windows.

The system model containing the DAMC modulation scheme control unit is illustrated in Figure 3, at a data rate  $R$  bps. The adaptive modulation is achieved based on the channel estimation,  $\hat{h}(r, t)$ , via the channel feedback path. We define  $r$  as the communication distance,  $T_s$  as the symbol duration, and  $t$  as the time to satisfy  $0 \leq t \leq T_s$ . The output of the control unit is fed into the multi-carrier modulator, which generates the transmitted signal,  $s(r, t)$ , given by

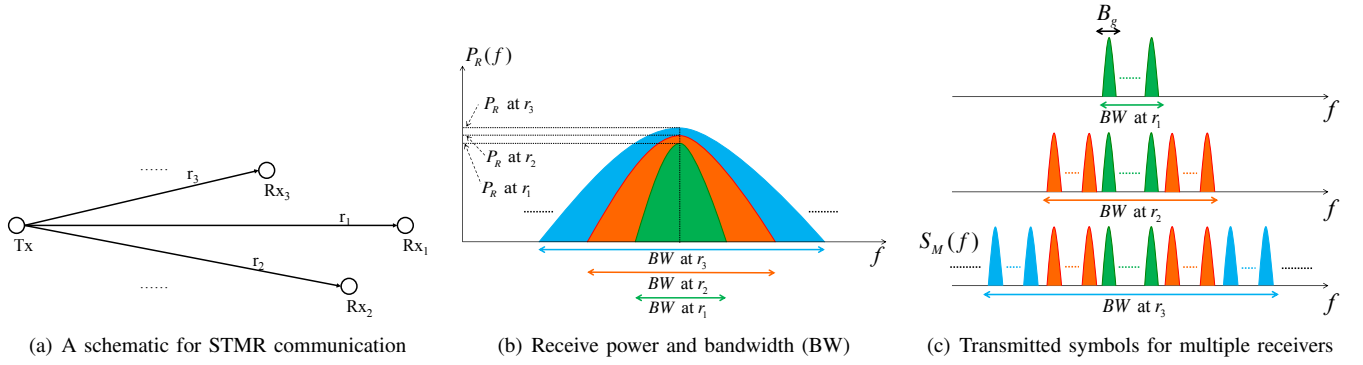
$$s(r, t) = \sum_{m=1}^{M(r)} \sum_{n=1}^{N_m} x_{mn}(r) g(t) \cos(2\pi f_{mn}(r)t + \phi_{mn}(r)), \quad (2)$$

where  $M$  refers to the total number of transmission windows that is distance-adaptive,  $N_m$  is the number of sub-windows in the  $m^{\text{th}}$  transmission window. In the  $n^{\text{th}}$  sub-window of the  $m^{\text{th}}$  window,  $x_{mn}$  denotes the complex symbol,  $f_{mn}$  is the carrier frequency and  $\phi_{mn}$  represents the phase offset.  $g(t)$  is a raised cosine pulse with rolloff factor  $\beta$ , which relates to the sub-window bandwidth  $B_g = \frac{1+\beta}{T_s}$ .

In the system model, the received signal,  $y(r, t)$ , is

$$y(r, t) = s(r, t) * h(r, t) + w(t), \quad (3)$$

where  $h$  is the Terahertz Band channel, and  $w$  denotes the total noise with power spectral density  $N_w$ , which includes the molecular absorption noise [7] and the thermal noise at the receiver, and satisfies  $P_w = \sum_{m=1}^{M(r)} \sum_{n=1}^{N_m} \int_{B_g} N_w$ .

Figure 4: STMR communication, with  $r_1 > r_2 > r_3 > \dots > r_V$ .

Next, we evaluate the performance of the DAMC scheme in the THz Band in terms of data rates. In STSR communication, all satisfying windows are allocated for transmission. The data rate,  $R$ , equals to the sum of the data rates on individual sub-windows,  $R_{mn}$ , as

$$R(r, P_b) = \sum_{m=1}^{M(r)} \sum_{n=1}^{N_m} R_{mn}(r, P_b), \quad (4)$$

where  $P_b$  stands for the targeted BER.

The channel gain on a sub-window is denoted by  $h_{mn}$ . We define  $\gamma_{mn} = h_{mn}^2 P_T / (B_g N_w)$ , and  $K = -1.5 / \ln(5P_b)$ . Since the channel information is known at the transmitter, the optimal water-filling strategy is adopted for power allocation. In our analysis, we apply the variable-rate variable-power MQAM modulation scheme, while other options are also possible. The optimal data rate that satisfies the targeted BER is expressed by

$$R(r, P_b) = B_g \sum_{m=1}^{M(r)} \sum_{n=1}^{N_m} \log \left( \frac{\gamma_{mn}}{\gamma_0 / K} \right), \quad (5)$$

where the power for each sub-window,  $P_{mn}$ , satisfies

$$\frac{P_{mn}}{P_T} = \begin{cases} \frac{1}{\gamma_0} - \frac{1}{K\gamma_{mn}} & \text{if } \gamma_{mn} \geq \gamma_0 / K \\ 0 & \text{if } \gamma_{mn} < \gamma_0 / K \end{cases} \quad (6)$$

and  $\sum_{m=1}^{M(r)} \sum_{n=1}^{N_m} P_{mn} \leq P_T$ . The cutoff fade depth,  $\gamma_0 / K$ , is

$$\sum_{m=1}^{M(r)} \sum_{n=1}^{N_m} \left( \frac{K}{\gamma_0} - \frac{1}{\gamma_{mn}} \right) = K. \quad (7)$$

More than one order of magnitude improvement in data rates can be achieved in the DAMC modulation scheme, at the costs of design complexity for the control unit, multi-carrier modulator and channel feedback path. The numerical analysis of the derived data rate is discussed in Section IV-A, in contrast with the single-band pulsed-based modulation as well as the fixed-bandwidth adaptive modulation.

### B. STMR Communication

For long-distance communication, much bandwidth in the THz Band is not being used, because of the high path loss and

small bandwidth in the transmission windows. For example at  $r = 10$  m, 4 THz-wide bandwidth is not being used. To better exploit the bandwidth in the THz Band, we advocate to allow simultaneous transmissions to multiple closer receivers, without compromising the transmission to long-distance receivers. We consider a THz Band communication network where there are one transmitter and  $V$  receivers. If  $r_v$  denotes the distance between the  $v^{\text{th}}$  receiver and the transmitter, Figure 4(a) illustrates the network with  $r_1 > r_2 > r_3 > \dots > r_V$ . In this section, we investigate the DAMC modulation scheme in STMR communication.

As the communication distance decreases, the path loss drops and as a result, the receive power and the available bandwidth are increased. By studying a transmission window in Figure 4(b), we have the following observations. On one hand, the transmission opportunities for long-distance communication are also useful for short distances, e.g., bandwidth for  $r_1$  is part of bandwidth for  $r_2$  and  $r_3$ . On the other hand, the sides of the transmission window can be used for short-distance communication, which do not affect the long-distance transmission using the center part of the window.

In light of these observations, the DAMC modulation scheme is used in STMR communication, by following the principle to accommodate long-distance communication first. In one transmission window, the resulting bandwidth occupation is illustrated in Figure 4(c), in which long-distance communication occupies the center of the transmission window first, while short-distance transmission uses the sides. As a result, the transmitted signal for multiple receivers in this transmission window in the frequency domain is illustrated as  $S_M(f)$ , where each sub-window has the bandwidth  $B_g$ .

This bandwidth allocation strategy closely interacts with the operation of the three steps in the design of the control unit in Figure 2. First, the channel characterization is performed for the long-distance communication first. Second, the transmission windows are allocated without interfering with the already occupied portion. Finally, the power and modulation on sub-windows are adaptively selected for each receiver.

By adopting this DAMC modulation scheme, the transmit-

ted signal in STMR communication,  $s_M(t)$ , is given by

$$s_M(t) = \sum_{v=1}^V \sum_{m=1}^{M^v} \sum_{n=1}^{N_m^v} x_{mn}^v g(t) \cos(2\pi f_{mn}^v t + \phi_{mn}^v), \quad (8)$$

where  $x_{mn}^v$ ,  $f_{mn}^v$ ,  $\phi_{mn}^v$  are the complex symbol, carrier frequency and phase designated for the  $v^{th}$  receiver. Moreover,  $M^v$  is the total number of transmission windows allocated for the  $v^{th}$  receiver, and  $N_m^v$  is the number of sub-windows in the  $m^{th}$  transmission window. After filtering out the unintended carriers, the signal at the  $v^{th}$  receiver,  $y^v(t)$ , is given by

$$y^v(t) = \sum_{m=1}^{M^v} \sum_{n=1}^{N_m^v} x_{mn}^v g(t) \cos(2\pi f_{mn}^v t + \phi_{mn}^v) * h(r_v, t) + w^v(t), \quad (9)$$

where  $h(r_v, t)$  is the channel response between the transmitter and the  $v^{th}$  receiver, and  $w^v$  is the additive white Gaussian noise with power spectral density  $N_w$ .

In STMR communication with  $V$  receivers satisfying  $r_1 > r_2 > r_3 > \dots > r_V$ , the total data rate,  $R_M$ , is equal to the sum of data rates for individual receivers, as

$$R_M(P_b) = \sum_{v=1}^V R^v(r_v, P_b), \quad (10)$$

where  $R^v(r_v, P_b)$  is the data rate of the link between the transmitter and the  $v^{th}$  receiver in the STMR network, which can be computed using (4) - (7) with  $M^v$  and  $N_m^v$ .

### C. Data Rates Comparison

The comparison of data rates in STSR and STMR communication is studied as follows. First,  $R^v(r_v, P_b)$  is less than  $R(r_v, P_b)$  in the STSR link obtained in (5), because the center of transmission windows for the  $v^{th}$  receiver are partially used by long-distance receivers. This relation is expressed as

$$R^v(r_v, P_b) \leq R(r_v, P_b), \text{ for } v = 1, 2, \dots, V. \quad (11)$$

Second,  $R_M(P_b)$  is bounded by  $R(r_1, P_b)$  and  $R(r_V, P_b)$ . On one hand, compared to the STSR link with  $r_1$ , the data rate is improved since additional bandwidth is used in STMR communication. On the other hand, the total number and bandwidth of transmission windows used for communication are dependent on the smallest distance, i.e.,  $r_V$ . Hence, in both STSR ( $r = r_V$ ) and STMR communication, the occupied bandwidth is equal. However, the centers of the transmission windows are occupied by long-distance links in STMR communication, which have worse path loss values compared to the STSR channel  $h(r_V, t)$ . Therefore, the inequalities are given by

$$R(r_1, P_b) \leq R_M(P_b) \leq R(r_V, P_b). \quad (12)$$

As a result, by using the DAMC scheme in STMR communication, the data rate can be further improved compared to the STSR case.

## IV. NUMERICAL ANALYSIS

In this section, we numerically evaluate the performance of the DAMC modulation scheme in terms of data rates, in both STSR and STMR communication regimes. Moreover, the achievable information rates of the single-band pulsed-based modulation [18] and fixed-bandwidth adaptive modulation [3] are analyzed in contrast with the DAMC scheme.

### A. Data Rates of STSR Communication

Figure 5(a) illustrates the data rate as a function of the distance in STSR communication. The transmit power  $P_T$  is equal to 1 dBm, the antenna gains are  $G_T = G_R = 30$  dB, and the noise power is  $P_w = -80$  dBm. As the distance rises, the channel path loss surges and hence, less transmission windows can be utilized and smaller data rates are achieved. In particular, the data rates of DAMC modulation scheme using variable-rate variable-power MQAM are plotted for targeted BER  $P_b = 10^{-3}, 10^{-6}, 10^{-9}$ , which are upper-bounded by the Shannon capacity. The selection of MQAM changes with distances, because of the variation of SNR over each sub-window. As the BER becomes stricter, the order of MQAM that can be supported by the same SNR drops and hence, the data rates shrink. Specifically, at  $r = 1$  m, the capacity reaches 10.49 Tbps, while data rates dwindle to 7.10 Tbps, 5.40 Tbps, and 4.63 Tbps for the three targeted BERs, respectively.

The interrelation between the data rates and the average SNR, is shown in Figure 5(b), for a fixed communication distance 1 m. The average SNR is computed as the mean of the received SNR on the available transmission windows. Specifically using the parameter values in Figure 5(a), the average SNR is 49.1 dB. Higher data rates are achieved with larger average SNR, e.g., the capacity reaches 11.18 Tbps at 50 dB. To compare the data rates of the DAMC scheme using adaptive MQAM with the Shannon capacity, a power loss of  $K$  is observed. Specifically, given targeted BERs  $P_b = 10^{-3}, 10^{-6}, 10^{-9}$ , additional 5.5, 9.1, 11.1 dB are needed for the DAMC scheme with adaptive MQAM to achieve the same rate.

Moreover, we compare the performance of the DAMC scheme with the single-band pulsed-based modulation and fixed-bandwidth adaptive modulation in terms of the achievable data rates in Figure 5(a), as follows.

First, the information rate of the single-band pulse-based modulation in [18] is numerically studied. At small distances (below 1 m), the THz Band channel have small path loss and the pulse can be transmitted without being distorted. Compared to the DAMC scheme, this information rate is less than 10 times worse, because with a similar aggregated bandwidth, the pulse-based modulation has maximum 1 bit/symbol while MQAM has  $\log_2(M)$  bits/symbol. At large  $r$ , the transmission windows are narrow, which drastically distorts the pulse and degrades the performance of the single-band modulation. By contrast, the DAMC scheme intelligently determine the transmit power and modulation over transmission windows, which can lead 2 orders of magnitudes advantage over the single-band pulse-based modulation. The results show that the data

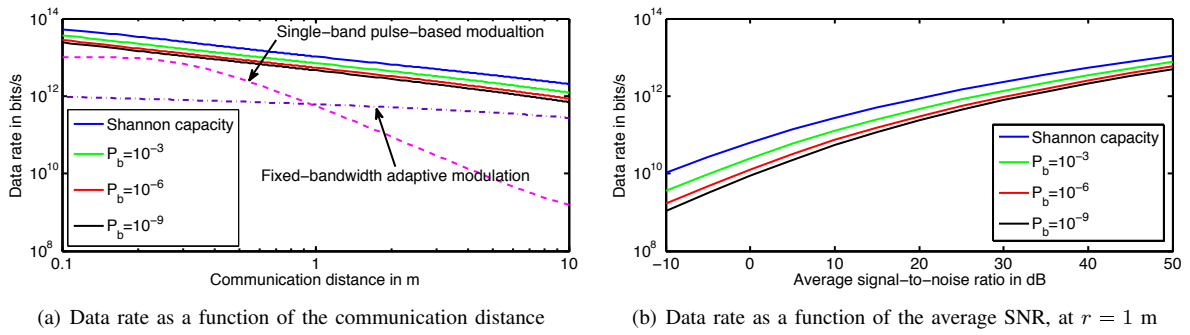


Figure 5: Data rates in STSR communication.

rate improvement is achieved particularly at large distances, at the costs of design complexity for the control unit, multi-carrier modulator and channel feedback path.

Second, we numerically analyze the achievable data rate of a fixed-bandwidth adaptive modulation, with the centered frequency at 0.35 THz and bandwidth of 51 GHz, as considered in [3]. Similar to the DAMC scheme, water-filling principle is used in this fixed-bandwidth adaptive modulation to compute the achievable data rate. For small communication distances, due to the restricted bandwidth, the achievable data rate of this fixed-bandwidth adaptive modulation is one order of magnitude less. For large distances, the bandwidth of transmission windows dwindles. Gradually, the difference of the two schemes wanes. Therefore, the DAMC scheme outperforms the fixed-bandwidth adaptive modulation, particularly at small distances.

### B. Data Rates of STMR Communication

In STMR communication, data rates are enhanced by utilizing the unused frequency bands without compromising the long-distance transmissions. In our analysis, we consider all the receivers are distant from the transmitter between 0.1 m and 10 m, i.e.,  $r_1 = 10$  m and  $r_V = 0.1$  m, where  $V$  is the number of receivers. Following the principle to accommodate the longer distance communication first, the DAMC modulation scheme is adopted to ameliorate the data rates.

In Figure 6(a), one transmitter communicates with two receivers at  $r_1 = 10$  m and  $r_2 = 0.1$  m. The THz Band is allocated for the long-distance receiver at  $r_1$  first, and then the unoccupied frequency bands are used to transmit to the receiver at  $r_2$ . Compared to the STSR case, one order of magnitude of data rates is enhanced by using the DAMC scheme in STMR communication. The data rates for the second receiver are less than  $R(0.1, P_b)$  in Figure 5(a). Moreover, the overall data rates in STMR communication are bounded by  $R(r_1, P_b)$  and  $R(r_2, P_b)$ . Hence, the inequalities (11) and (12) are satisfied.

Alternatively, Figure 6(b) illustrates the impact of the number of receivers on data rates for a fixed targeted BER  $10^{-6}$ . In this study, receivers are logarithmically uniformly located, e.g., distances are 0.1, 1, 10 m for  $V = 3$ . The

observations are summarized as follows. First, by exploiting unused bandwidth, simultaneous transmissions to multiple receivers increase data rates. Second, as more receivers are in the network, the allocated bandwidth for each receiver is reduced and hence, the slope of increase on data rates lessens. Third, as more receivers are in the network, much bandwidth is occupied by long-distance receivers in the DAMC modulation scheme. These receivers have large path loss values and hence, the total data rates in STMR communication abate. Hence, the balance between the number of receivers that can be simultaneously supported and the total data rates need to be further investigated.

### V. CONCLUSION

Terahertz Band (0.1–10 THz) communication is envisioned to meet the demand for ultra-broadband wireless communication. THz Band communication will address the spectrum scarcity and capacity limitations of current cellular systems, and enable a plethora of applications both in classical networks and novel nanoscale networks.

In this paper, we have developed a novel DAMC modulation scheme for both STSR and STMR cases in THz Band communication. The developed DAMC scheme takes advantage of the distance- and frequency-dependent channel peculiarities, and provides adaptive utilization of the ultra-broad bandwidth in the THz Band. Moreover, we have analytically and numerically investigated the data rate of the DAMC scheme, as a function of the targeted bit error rate, average signal-to-noise ratio and number of receivers. We have compared the performance of the DAMC scheme in contrast with the single-band pulse-based modulation and fixed-bandwidth adaptive modulation.

The results show that the DAMC modulation scheme can provide up to several Tbps data rates over 10 m, which outperforms existing single-band pulse-based modulation and fixed-bandwidth adaptive modulation by more than one order of magnitude. Furthermore, compared to the STSR case, one order of magnitude of data rates can be enhanced by using the DAMC scheme in STMR communication. However, these improvements by using the DAMC modulation scheme are at the costs of design complexity for the control unit, multi-carrier modulator and channel feedback path.

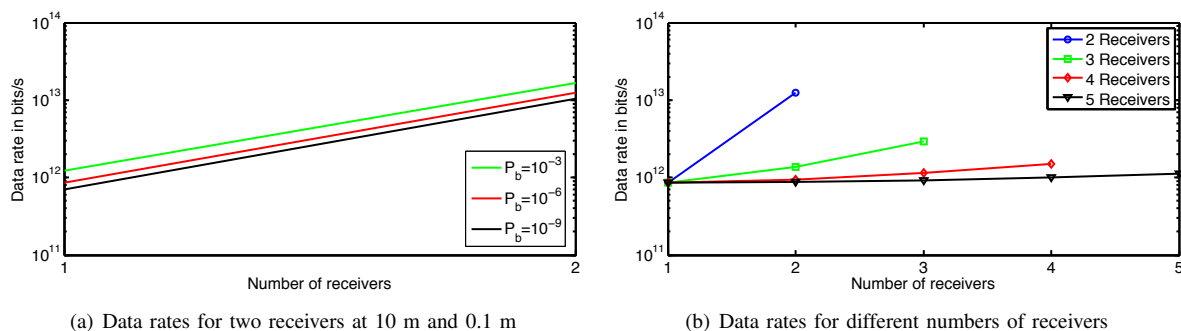


Figure 6: Data rates in STMR communication.

## ACKNOWLEDGEMENT

The authors would like to thank Dr. Josep Miquel Jornet for his constructive criticism, which helped to improve the quality of the paper.

This work was supported by the U.S. National Science Foundation (NSF) under Grant No. CCF-1349828.

## REFERENCES

- [1] S. Cherry, "Edholm's Law of Bandwidth," *IEEE Spectrum*, 2004.
- [2] M. Koch, "Terahertz Communications: A 2020 Vision," *Terahertz Frequency Detection and Identification of Materials and Objects*, 2007.
- [3] R. Piesiewicz, T. Kleine-Ostmann, N. Krumbholz, D. Mittleman, M. Koch, J. Schoebel, and T. Kurner, "Short-range Ultra-broadband Terahertz Communications: Concepts and Perspectives," *IEEE Antennas and Propagation Magazine*, vol. 49, no. 6, pp. 24–39, 2007.
- [4] H. Song and T. Nagatsuma, "Present and Future of Terahertz Communications," *Terahertz Science and Technology, IEEE Transactions on*, vol. 1, no. 1, pp. 256–263, 2011.
- [5] T. Rappaport, J. Murdock, and F. Gutierrez, "State of the Art in 60-GHz Integrated Circuits and Systems for Wireless Communications," *Proceedings of the IEEE*, vol. 99, no. 8, pp. 1390–1436, 2011.
- [6] G. R. Aiello and G. D. Rogerson, "Ultra-Wideband Wireless Systems," *IEEE Microwave Magazine*, vol. 4, no. 2, pp. 36–47, 2003.
- [7] J. Jornet and I. Akyildiz, "Channel Modeling and Capacity Analysis for Electromagnetic Wireless Nanonetworks in the Terahertz Band," *IEEE Transactions on Wireless Communications*, vol. 10, no. 10, 2011.
- [8] M. Wolf and D. Kreß, "Short-range Wireless Infrared Transmission: The Link Budget Compared to RF," *IEEE wireless communications*, 2003.
- [9] T. Nagatsuma, H. Ito, and T. Ishibashi, "High-Power RF Photodiodes and Their Applications," *Laser & Photonics Reviews*, vol. 3, no. 1-2, pp. 123–137, 2009.
- [10] K.-C. Huang and Z. Wang, "Terahertz Terabit Wireless Communication," *IEEE Microwave Magazine*, vol. 12, no. 4, pp. 108–116, Jun. 2011.
- [11] E. Ojefors, B. Heinemann, and U. Pfeiffer, "Subharmonic 220- and 320-GHz SiGe HBT Receiver Front-ends," *IEEE Transactions on Microwave Theory and Techniques*, vol. 60, no. 5, pp. 1397–1404, 2012.
- [12] M. Micovic, A. Kurdoghlian, A. Margomenos, D. Brown, K. Shinohara, S. Burnham, I. Milosavljevic, R. Bowen, A. Williams, P. Hashimoto *et al.*, "92–96 GHz GaN Power Amplifiers," in *IEEE MTT-S International Microwave Symposium Digest*, 2012, pp. 1–3.
- [13] T. Otsuji, S. Tombet, A. Satou, H. Fukidome, M. Suemitsu, E. Sano, V. Popov, M. Ryzhii, and V. Ryzhii, "Graphene-based devices in terahertz science and technology," *Journal of Physics D: Applied Physics*, vol. 45, no. 30, p. 303001, 2012.
- [14] J. M. Jornet and I. F. Akyildiz, "Graphene-based Plasmonic Nano-antennas for Terahertz Band Communication in Nanonetworks," *to appear in IEEE Journal of Selected Topics in Communications*, 2013.
- [15] T. Kleine-Ostmann and T. Nagatsuma, "A review on terahertz communications research," *Journal of Infrared, Millimeter and Terahertz Waves*, vol. 32, no. 2, pp. 143–171, 2011.
- [16] M. Tonouchi, "Cutting-edge Terahertz Technology," *Nature photonics*, vol. 1, no. 2, pp. 97–105, 2007.
- [17] I. Akyildiz, J. Jornet, and C. Han, "Terahertz Band: Next Frontier for Wireless Communications," *to appear in Physical Communication (Elsevier) Journal*, 2013.
- [18] J. M. Jornet and I. F. Akyildiz, "Information Capacity of Pulse-based Wireless Nanosensor Networks," in *Proc. of the 8th Annual IEEE Communications Society Conference on Sensor, Mesh and Ad Hoc Communications and Networks, SECON*, Jun. 2011.
- [19] R. C. Daniels and R. W. Heath, "60 GHz Wireless Communications: Emerging Requirements and Design Recommendations," *IEEE Vehicular Technology Magazine*, vol. 2, no. 3, pp. 41–50, 2007.
- [20] T. Keller and L. Hanzo, "Adaptive Multicarrier Modulation: A Convenient Framework for Time-Frequency Processing in Wireless Communications," *Proceedings of the IEEE*, vol. 88, no. 5, pp. 611–640, 2000.
- [21] T. Ohtsuki, "Multiple-Subcarrier Modulation in Optical Wireless Communications," *IEEE Communications Magazine*, vol. 41, no. 3, pp. 74–79, 2003.